A DAMAGE MECHANICS BASED FAILURE MODEL FOR DYNAMIC IMPACT ON COMPOSITE LAMINATES

Mauricio V. Donadon
Department of Aeronautics, Imperial College London, South Kensington, London, SW7 2AZ, U.K
mauricio.donadon@imperial.ac.uk

Sérgio Frascino Müller de Almeida
Department of Mechanical Engineering, Instituto Tecnologico de Aeronáutica
São José dos Campos-SP, Brazil
frascino@ita.br

Abstract. *This paper presents an energy based damage model for predicting the dynamic material response of composite laminates under impact loading. The formulation is based on the Continuum Damage Mechanics (CDM) approach and enables the control of the energy dissipation associated with each failure mode regardless of mesh refinement and fracture plane orientation. Internal thermodynamically irreversible damage variables were defined in order to quantify damage concentration associated with each possible failure mode and predict the gradual stiffness reduction during the impact damage process. The material model has been implemented into LS-DYNA3D explicit finite element code and it has proven to be capable of reproducing experimental results with good accuracy in terms of static/dynamic responses, absorbed energy and damage extension.*

Keywords*: Composites, impact dynamics, damage mechanics, finite elements*

1. Introduction

The popularity of composites has growth over the years due to the superior physical and chemical properties they exhibit over metals or metal alloys. Composite structures have a high strength-to-weight and stiffness-to-weight ratio, good fatigue and corrosive properties, fewer part count and radar avoidance properties that make them attractive for stealth applications. However, laminated polymer composite structures do have their drawbacks which include poorer performance at high temperatures, poor through-the-thickness properties and poor performance under transverse impact.

Impact on composites can be generally classified into two categories, namely *low* and *high velocity impacts*; however, there is not a clear transition between these categories and authors disagree on their definition. Examples of these two categories are accidental dropping of tools during maintenance and ballistic impact experienced at the battlefield, respectively. According to Davies and Robinson (1992), *low velocity impacts* are impact where through thickness stress wave plays no significant role in the stress distribution, with impact velocities ranging from 10 to 20 m/s. An alternative definition is proposed by Abrate (1991), where *low velocity impacts* occur for impact speed of less than 100 m/s. The term *high velocity impact* can be used to describe impact velocities ranging from 100 to 70 km/s, Davies and Olsson (2004).

Laminated composites respond differently to high and low velocity impacts. For low velocity impacts the contact duration is sufficiently long for the entire structure to respond to the impact and energy is absorbed elastically and/or eventually in damage creation/propagation whereas for high velocity the impact event duration is so short that the structure may have no time to respond in flexural or shear modes, and the main issue will be whether complete penetration occurs or not (Davies and Olsson, 2004). The resulting damage mechanisms due to impact loading can be divided into four distinct damage categories: delamination, matrix cracking, fibre breakage and total perforation. Under low velocity impacts, the resulting type of damage in the laminated composite follows the previous sequence as the impact energy is increased, whereas for high velocity impacts, damage is almost exclusively perforation with a surrounded delaminated area around the hole.

Some analytical approaches have been proposed in the literature to model such complex phenomena (Abrate, 2001; Olsson, 2001; Olsson et al, 2005). However, these approaches are restricted to simple impact cases where the target is relatively small and complicating factors such as transverse shear deformation and rotary inertia do not play any significant role. Also, they neither describe the impactor nor the plate geometries, and the contact is assumed to be localized at a single point of the structure. The stiffness values depend on analytical solutions for particular plate geometries, loadings and boundary conditions which makes the strategy very limited. In order to overcome such limitations, generalized numerical models are required. The finite element method has become the most popular numerical method for impact modeling in both research and industrial environments. Different commercial finite element codes have been used for impact simulation in recent years such as ABAQUS, LSDYNA-3D among others. These codes have advanced contact logics to deal with a wide range of contact problems as well as a variety of beam, plate, shell and solid finite element formulations implemented. Also, they allow the implementation of user defined subroutines which can be customized for particular applications.

The material model plays a crucial role in the impact damage modeling, controlling the damage extension, absorbed energy, stiffness reduction and final dynamic structural behaviour.

Different approaches are currently available in the literature for damage modeling in composite laminates and they can be broadly divided into four categories: failure criteria, fracture mechanics, plasticity and damage mechanics approaches, respectively. Failure criteria approach was initially developed to unidirectional materials and restricted static regime. Interactive and non-interactive polynomial expressions either in terms of strains or stresses can be used to define the so-called *failure envelope* for the material under investigation (Jones, 1999). The disadvantage in using the failure criteria approach for composite materials is that neither the position nor the crack sizes can be predicted; the fracture mechanics approach may be more attractive for this reason. Fracture mechanics approach considers the strain energy at the front of a crack of a known size and compares it with critical quantities such as critical strain energy release rate. The approach has been successfully applied to predict residual compression strength and delamination growth in composites, (Matthews et al, 2000; Crisfield et al, 1998). Despite its attractiveness, the fracture mechanics approach cannot be easily incorporated into a progressive failure methodology because its application requires an initial flaw. Plasticity approach is suitable for composites that exhibit ductile behaviour such as Boron/Aluminium, Graphite/PEEK and other thermoplastic composites and it can be combined with the failure criteria approach for damage prediction (Olsson et al, 1992). The Continuum Damage Mechanics (CDM) approach has been investigated by many researchers in recent years and its application to impact damage modeling has shown to be very efficient. The method was originally developed by Kachanov (1958) and Rabotnov (1968) and it has the potential to predict different composite failure modes such as matrix cracking, fibre fracture and delamination. Recent works using such an approach for impact damage modelling include works by Ladeveze and Dantec (1992), Johnson (2001), Williams et al (2003), Iannucci (2004) and Donadon et al (2004a). The advantage of the CDM approach is that it can be easily combined with a stress and/or strain failure criteria for predicting damage initiation and fracture mechanics approach for the failure progression by coupling the internal damage variables with the fracture energy.

This paper presents a progressive failure model based on the Continuum Damage Mechanics (CDM) approach. The formulation enables the control of the energy dissipation associated with each failure mode (matrix cracking in tension/compression, fibre failure in tension/compression and shear failure) regardless of mesh refinement, element topology and fracture direction by using an advanced mesh insensitivity algorithm. The material model was implemented into LS-DYNA3D explicit finite element code with solid elements. Composite panels were manufactured using a *Resin Infusion under Flexible Tooling* (*RIFT*) *Process* setup proposed by Donadon et al (2004b) and tested under impact loading using an instrumented drop test tower. Good correlations between experimental and numerical results for static and dynamic impact tests on X-ply laminates were obtained.

2. Damage model formulation

The damage model proposed here is based on the Continuum Damage Mechanics (CDM) approach and it is based on the following assumptions:

- Cracks are assumed to be smeared over a Representative Volume Element (RVE) of the material;
- Five internal damage variables, $d_{ij}^{k} \in [0,1]$ were introduced at the lamina level to quantify the crack concentration in the fractured cross-sectional are of the RVE. The subscripts i and j refer to the material local coordinate system, being $i, j = 1$ for fibre fracture and $i, j = 2$ for matrix cracking. The superscript k refers to the type of failure, where $k = t$ and $k = c$ for tension and compression failure, respectively. Three extra d_{ij} damage variables were introduced to quantify damage due to shear loadings. Maximum strain failure criterion is used to detect failure initiation in tension/compression in the fibre direction, tension in the matrix direction and in-plane shear failure. A stress based criterion proposed by Puck and Shurmann (2002) is used to detect transverse compression failure;
- The damage evolution laws are based on strains with their ultimate strain values defined as a function of the fracture energies per unit of volume of damaged material.

The idea behind the smeared cracking models is to relate the specific or volumetric energy, which is defined by the area underneath the stress-strain curve, with the fracture energy of the material. In order to do so, a methodology proposed by Bazant (1983), which was originally developed for concrete has been used in this work. The method assumes a strain softening constitutive law for modeling the gradual stiffness reduction due to the micro-cracking process within the cohesive zone or process zone. Using the CDM approach damage growth can be directly coupled to the fracture energy by introducing a parameter defined as characteristic length. This parameter is related to size of the process zone within the fractured region of the material under investigation.

Based on the principle of the strain equivalence (Chaboche, 1988), which states that a *damaged material under the nominal stress* s *shows the same stress strain response as comparable undamaged material under the effective stress*

$\bar{s}$ in conjunction with the additive strain decomposition, the following explicit incremental material orthotropic relationship can be obtained,

$$\Delta\sigma = \mathbf{E}\,(\mathbf{d}(\Delta e - \Delta e^{in}) - \Delta\mathbf{d}(e - e^{in})) \tag{1}$$

with,

$$\mathbf{E} = \frac{1}{\Omega}\begin{bmatrix} E_{11}(1-n_{23}n_{32}) & E_{22}(n_{12}-n_{32}n_{13}) & E_{33}(n_{13}-n_{12}n_{23}) & 0 & 0 & 0 \\ E_{11}(n_{21}-n_{31}n_{23}) & E_{22}(1-n_{13}n_{31}) & E_{33}(n_{23}-n_{21}n_{13}) & 0 & 0 & 0 \\ E_{11}(n_{31}-n_{21}n_{32}) & E_{22}(n_{32}-n_{12}n_{31}) & E_{33}(1-n_{12}n_{21}) & 0 & 0 & 0 \\ 0 & 0 & 0 & G_{23} & 0 & 0 \\ 0 & 0 & 0 & 0 & G_{31} & 0 \\ 0 & 0 & 0 & 0 & 0 & G_{12} \end{bmatrix} \tag{2}$$

$$\mathbf{d} = \begin{bmatrix} (1-d_{11}^k) & (1-d_{22}^k) & 1 & 0 & 0 & 0 \\ (1-d_{11}^k) & (1-d_{22}^k) & 1 & 0 & 0 & 0 \\ (1-d_{11}^k) & (1-d_{22}^k) & 1 & 0 & 0 & 0 \\ 0 & 0 & 0 & (1-d_{23}) & 0 & 0 \\ 0 & 0 & 0 & 0 & (1-d_{31}) & 0 \\ 0 & 0 & 0 & 0 & 0 & (1-d_{12}) \end{bmatrix}, \quad \Delta\mathbf{d} = \begin{bmatrix} \Delta d_{11}^k & \Delta d_{22}^k & 0 & 0 & 0 & 0 \\ \Delta d_{11}^k & \Delta d_{22}^k & 0 & 0 & 0 & 0 \\ \Delta d_{11}^k & \Delta d_{22}^k & 0 & 0 & 0 & 0 \\ 0 & 0 & 0 & \Delta d_{23} & 0 & 0 \\ 0 & 0 & 0 & 0 & \Delta d_{31} & 0 \\ 0 & 0 & 0 & 0 & 0 & \Delta d_{12} \end{bmatrix} \tag{3}$$

$$\Omega = 1 - n_{12}n_{21} - n_{23}n_{32} - n_{31}n_{13} - 2n_{21}n_{32}n_{13} \tag{4}$$

where Δs is the stress increment vector, $\mathbf{E}$ is the undamaged orthotropic stiffness matrix, $\mathbf{d}$ and $\Delta\mathbf{d}$ are defined as damage and incremental damage matrices, respectively. e and e^{in} are the total and inelastic strains and Δe, Δe^{in} their correspondent increments, respectively. The Poisson's ratio must be reduced in a similar manner to the Young's module to preserve the positive definiteness of the material stress-strain law, therefore

$$\frac{n_{ij}(1-d_{ii}^k)}{E_{ii}(1-d_{ii}^k)} = \frac{n_{ji}(1-d_{jj}^k)}{E_{jj}(1-d_{jj}^k)} \tag{5}$$

The inelastic strain components are associated with the non-linear material behaviour in shear, which results in irreversible strains due to partial crack closure within the RVE. A polynomial cubic stress-strain relationship was used to represent the non-linear behaviour in shear which is given by (Donadon et at, 2004):

$$t_{ij}(g_{ij}) = c_1 g_{ij}^3 + c_2 g_{ij}^2 + c_3 g_{ij} \tag{6}$$

where the c_1, c_2 and c_3 are determined by fitting the polynomial expression with the experimental stress-strain curves. The inelastic strain components are obtained from the strain additive decomposition ($g_{ij} = g_{ij}^e + g_{ij}^{in}$) and they are given by,

$$g_{ij}^{in} = g_{ij} - \frac{t_{ij}}{G_{ij}^0(1-d_{ij})} \tag{7}$$

where g_{ij}, d_{ij} and G_{ij}^0 are the total shear strain, shear damage variable and initial undamaged shear stiffness, respectively. In order to detect damage initiation the following strain based criterion is used (Donadon et at, 2004),

$$F_{ij}^s(g_{ij}) = \left(\frac{g_{ij}}{g_{ij}^0}\right)^2 - 1 \geq 0 \tag{8}$$

where g_{ij}^0 is defined as limit strain in shear. The matrix micro-cracking process starts when the shear strain exceeds that limit and after detecting damage initiation, the damage progression in shear is assumed to be driven by strains with a damage evolution law given as follows (Donadon et at, 2004),

$$d_{ij}(g_{ij}) = l_1(g_{ij}) + l_2(g_{ij}) - l_1(g_{ij})l_2(g_{ij}) \tag{9}$$

where functions $l_1(g_{ij})$ and $l_2(g_{ij})$ are defined as

$$\left.\begin{aligned} l_1(g_{ij}) &= 1 - a g_{ij} \\ l_2(g_{ij}) &= 0 \end{aligned}\right\} \text{for } g_{ij}^0 \le g_{ij} \le g_{ij}^f \quad \text{and} \quad \left.\begin{aligned} l_1(g_{ij}) &= 1 - a g_{ij}^f \\ l_2(g_{ij}) &= \frac{g_{ij}^{\max}}{g_{ij}^{\max} - g_{ij}^f}\left(1 - \frac{g_{ij}^f}{g_{ij}}\right) \end{aligned}\right\} \text{for } g_{ij}^f \le g_{ij} \le g_{ij}^{\max} \tag{10}$$

The strain terms g_{ij}^f and $g_{ij}^{\max}$ correspond to the failure strain and maximum strain, respectively and a is a material constant which can be obtained by measuring the gradual shear stiffness reduction in cyclic loading-unloading shear testing using $(+45/-45)_n$ specimens. The maximum strain is the strain in which the material is fully damaged and its magnitude depends on the amount of energy to be dissipated in shear and it can be computed from,

$$g_{ij}^{\max} = \frac{2}{t_{ij}(g_{ij}^f) l_{ij}^s}\left[G_{fij}^s - \int_0^{g_{ij}^f} t_{ij}(g_{ij}) dg_{ij}\right] + g_{ij}^f \tag{11}$$

where G_{fij}^s is the shear fracture energy and l_{ij}^s is the characteristic length associated with shear failure.

Damage initiation due to tensile loading in the fibre and matrix directions is predicted using a strain based failure criteria given in the following form,

$$F_{ij}^t(e_{ij}) = \left(\frac{e_{ij}}{e_{ij}^f}\right)^2 - 1 \ge 0 \tag{12}$$

where e_{ij}^f values correspond to the failure strains either for fibre or matrix failure, depending on the considered local direction. Damage evolution is given as a function of strains as follows,

$$d_{ij}^t(e_{ij}) = \frac{e_{ij}^{\max}}{e_{ij}^{\max} - e_{ij}^f}\left(1 - \frac{e_{ij}^f}{e_{ij}}\right) \qquad \text{with,} \qquad e_{ij}^{\max} = \frac{2G_{fij}^t}{s_{ij}^f l_{ij}^t} \tag{13}$$

where G_{fij}^t, s_{ij}^f and l_{ij}^t are the fracture energy, tensile strength and characteristic length for fibre/matrix failure in tension, respectively. For failure initiation due to transverse compression a stress based failure criterion proposed by Puck and Shurmann (2002) has been used. The failure criterion is based on the Mohr-Coulomb failure theory and it is given by

$$F_{22}^c(s_{nt}, s_{nl}) = \left(\frac{s_{nt}}{S_{23} + m_{nt} s_{nn}}\right)^2 + \left(\frac{s_{\ln}}{S_{12} + m_{\ln} s_{nn}}\right)^2 \ge 1 \tag{14}$$

where the subscripts n, l and t refer to the normal and tangential directions, respectively, in respect to fracture plane direction. S_{23} and S_{12} are the transverse and in-plane shear strengths, respectively. Using a quadratic stress based failure criterion proposed by Hashim (1980) it is possible to show that the fracture plane orientation with respect to the through thickness direction for unidirectional transverse compression loading can be written as,

$$q_f = \cos^{-1}\sqrt{w} \tag{15}$$

with $w = (-B \pm \sqrt{B^2 + 4A})/2A$ where $B = (Y_c / S_{23})^2$ and $A = [1 - B^2]$. Y_c and S_{23} are the transverse strengths in compression and shear, respectively. The strength ratio Y_c / S_{23} is typically around 2 for unidirectional composites (Jones, 1999); two possible solution for the fracture plane are obtained by substituting this value into Eq. (15): $q_f = 0^0$ and $q_f = 54.7^0$, respectively. Both these solutions are mathematically admissible, however; the only one physically

consistent is $q_f = 54.7^0$ which agrees very well with experimentally observed values which vary between 53^0 and 54^0 according to Puck and Shurmann (2002). The idea behind Puck and Shurmann (2002) failure criterion is that the stress components acting on the fracture plane must be compared to the strengths of their action plane and not just to the nominal measured strengths from conventional mechanical tests. It also states that the normal stress acting on the fracture plane, makes no contribution towards initiating the failure. On the contrary, it impedes the shear fracture caused by the shear stresses s_{nt} and $s_{\ln}$ by giving rise to additional resistance to shear fracture and this resistance increases as a function of the normal compressive stress s_{nn}. Following the Mohr-Coulomb failure theory the friction coefficients can be determined as a function of the material friction angle as follows,

$$m_{nt} = \tan f = \tan(2q_f - 90^0), \qquad \frac{m_{nt}}{S_{23}} = \frac{m_{\ln}}{S_{12}} \tag{16}$$

Having determined the direction of the fracture plane, the stresses/strains are rotated to that direction and Eq. (14) is then applied to detected damage initiation. It would be reasonable to assume damage growth as a function of the combined local tangential shear strain state at the fracture plane and by doing so, one can write a damage evolution law in the following form,

$$d_{22}^c(g_{nt}, g_{\ln}) = \frac{g_r^{\max}}{g_r^{\max} - g_r^f}\left(1 - \frac{g_r^f}{g_r}\right) \qquad \text{with,} \quad g_r = \sqrt{g_{nt}^2 + g_{\ln}^2} \quad \text{and} \quad g_r^{\max} = \frac{2G_{f22}^c}{\sqrt{s_{nt}^2 + s_{\ln}^2}\, l_{22}^c} \tag{17}$$

where g_r^f is the resultant shear failure strain when $F_{22}^c(s_{nt}, s_{nl}) = 1$ and $g_r^{\max}$ is given in terms of the fracture energy in compression G_{f22}^c and the characteristic length l_{22}^c. The resultant local degraded stress tensor is then given by

$$[s_{ij}]_{nlt} = [s_{ij}(q_f)] = \begin{bmatrix} s_{tt} & s_{nt}(1-d_{22}^c) & s_{lt} \\ s_{nt}(1-d_{22}^c) & s_{nn} & s_{nl}(1-d_{22}^c) \\ s_{lt} & s_{nl}(1-d_{22}^c) & s_{ll} \end{bmatrix} \tag{18}$$

After being degraded, the stresses are then rotated back to the local lamina coordinate system.

For fibre failure in compression, a maximum strain failure criteria given in the following form has been used,

$$F_{11}^c(e_{11}) = \frac{e_{11}}{e_{11}^f} - 1 \geq 1 \tag{19}$$

where e_{11}^f is the failure strain in compression. In order to model the fibre kinking propagation a kind of reverse crack approach has been adopted in which the damage growth law assumes a similar form as the one used for predicting damage due to fibre failure in tension, that is,

$$d_{11}^c = \frac{e_{11}^{\max}}{e_{11}^{\max} - e_{11}^f}\left(1 - \frac{e_{11}^f}{e_{11}}\right) \qquad \text{with,} \qquad e_{11}^{\max} = \frac{2G_{f11}^c}{s_{11}^f l_{11}^c} \tag{20}$$

where G_{f11}^c is the fracture energy required for fibre kinking propagation and l_{11}^c is the characteristic length in compression, which is assumed to be the same as the one for tension. In order to simulate matrix crushing and fragments interaction effects within the crushing zone of the material, the direct stress s_{11} is degraded to a minimum residual stress which has been defined as $s_{11}^{res} = 0.10 s_{11}^f$.

2.1. Objectivity algorithm

In order to control the energy dissipation within a single finite element and ensure the objectivity of the model, an algorithm originally proposed by Oliver (1989) has been extended to handle orthotropic materials. The methodology enables the energy control for each failure mode regardless of mesh refinement, element topology and crack propagation direction. Firstly a set of bcal Cartesian axes x,y is defined at the centre of the element where the integration point is located, this being identified by the values of the isoparametric coordinates $(x,h,z) = (0,0,0)$ (see

Fig.1). The direction of the local axis x' is then defined by the normal to the fracture plane, which is equal to the fibre angle for fibre failure $(q_j = q_{fibre})$ and $(q_j = q_{fibre} + 90^0)$ for matrix failure.

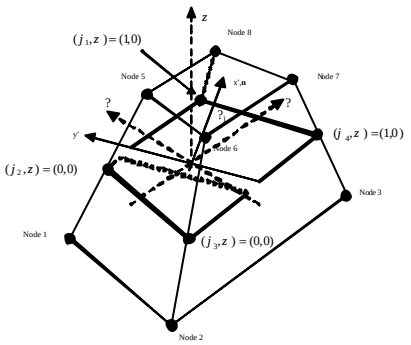

Figure 1. Determination of the characteristic length for 8-nodes hexahedron solid elements

A differentiable function $j(x,h)$ with continuity C^0 is introduced to describe the crack displacement gradient within the cracked band of elements, which assumes values $j_i = 1$ if $x' \geq 0$, otherwise $j_i = 0$. Having this function defined is possible to demonstrate that the characteristic length for hexahedron elements is given by (Oliver, 1989)

$$l_{ij}^k(x_j,h_j) = \left(\frac{\partial j(x_j,h_j)}{\partial x'} \right)^{-1} = \left(\sum_{i=1}^{4} \left[\frac{\partial N_i(x_j,h_j)}{\partial x} \cos(q_j) + \frac{\partial N_i(x_j,h_j)}{\partial y} \sin(q_j) \right] j_i \right)^{-1} \quad (22)$$

where $N_i(x_j,h_j)$ is linear interpolation function between two virtual nodes at the mid-plane of the element. A similar procedure is applied to handle transverse fracture in which the function $j(x,h)$ is replaced by $j(x,z)$.

3. Results and discussions

Composite panels were manufactured using RIFT and tested according to internationally recognized standards, under uniaxial tension/compression in the transverse and longitudinal directions, respectively. Details about the manufacturing setup are given by Donadon et al (2004b). A cyclic $(+45/-45)_n$ in-plane shear testing was carried out to characterize the material behaviour in shear. In order to obtain the fracture energies associated with each failure mode, intralaminar fracture toughness tests were undertaken using three different pre-cracked geometries, namely Overhead Compact Tension (OCT) (Tension/Compression), Double Edge Notch (DEN)(Tension) and Four-point-Bending specimens (Donadon et al, 2005). The experimentally obtained mechanical properties are summarized in Tab. 1.

Table 1. Mechanical properties

E_{11} [GPa]	E_{22} [GPa]	$G_{12}=G_{23}=G_{31}$ [GPa]	n_{12}	e_{11}^f (tension) [%]	e_{11}^f (compression) [%]	e_{22}^f (tension) [%]	$S_{12}=S_{23}$ [MPa]	Y_c [MPa]
100.0	8.11	4.65	0.33	1.8	0.8	0.7	61	160

Fracture energies [KJ/m^2]				
G_{f11}^t	G_{f11}^c	G_{f22}^t	G_{f22}^c	$G_{f12}^s = G_{f31}^s = G_{f23}^s$
100.0	18.0	2.5	2.0	2.0

3.1 Coupon tests simulations

The finite element models for uniaxial tension in the longitudinal and transverse directions had dimensions of $200 \times 20 \times 1.35\text{mm}^3$ and $200 \times 20 \times 2.25\text{mm}^3$, respectively with a gauge length equals to 100mm for both models. The corresponding lay-ups for the longitudinal and transverse uniaxial tensile tests were $(0^0)_3$ and $(90^0)_5$, respectively. For compression test simulations the dimensions of the virtual coupons were $90 \times 20 \times 1.35\text{mm}^3$ and $90 \times 20 \times 2.25\ \text{mm}^3$, with a gauge length equals to 10mm for both specimens and $(0^0)_5$ and $(90^0)_5$ lay-ups for longidudinal and transverse compression directions, respectively. The virtual coupon for in-plane shear testing had dimensions of $200 \times 20 \times 2.7\ \text{mm}^3$ and $(+45/-45)_3$ layup. Each ply with a nominal thickness of 0.45mm were individually modeled for each coupon test using 8 nodes hexahedron single integration solid elements available in LS-DYNA3D. A stiffness based hourglass algorithm was used to avoid the formation of anomalous hourglass modes arising from the use of under integrated elements. Due to the explicit dynamic nature of the finite element code the simulation was carried out quasi-statically

using a dynamic relaxation method. Comparisons between numerical and experimental results for tension, compression and in-plane shear are presented and Figs. 2, 3 and 4, respectively. The depicted failure modes are typical of each test.

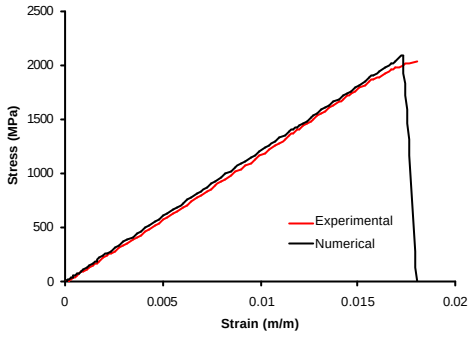

(a) Longitudinal Stress-Strain response in Tension

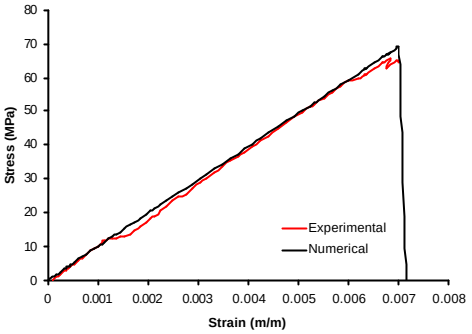

(b) Transverse Stress-Strain response in Tension

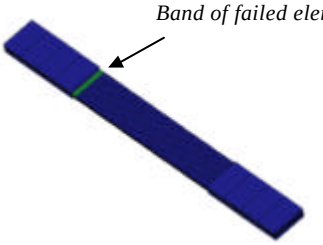

Experimental fracture location for transverse tensile specimens

Figure 2. Comparison between experimental and numerical predictions for tensile coupon tests

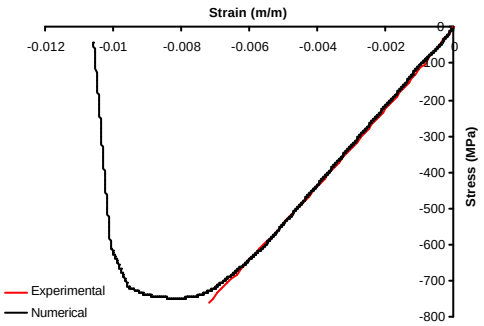

(a) Longitudinal Stress-Strain response in Compression

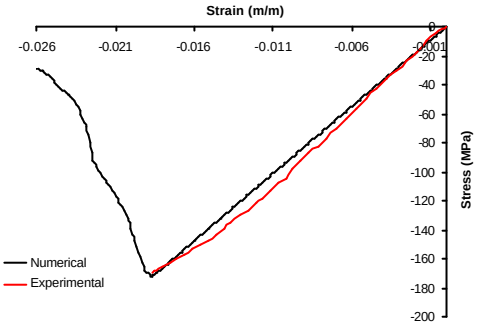

(b) Transverse Stress-Strain response in Compression

Experimental fracture location for longitudinal compression specimens

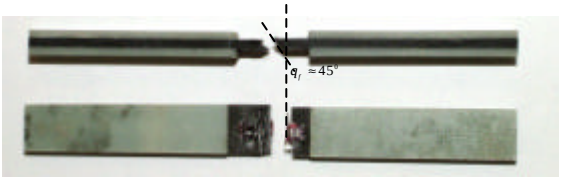

Experimental fracture location for transverse compression specimens

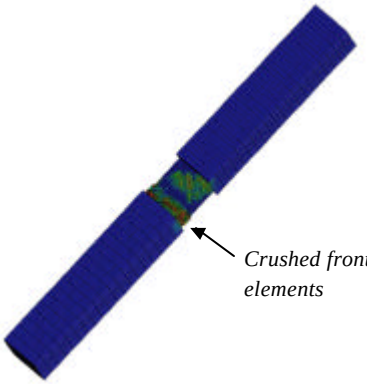

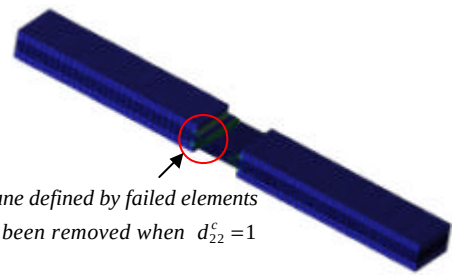

Figure 3. Comparison between experimental and numerical predictions for compression coupon tests

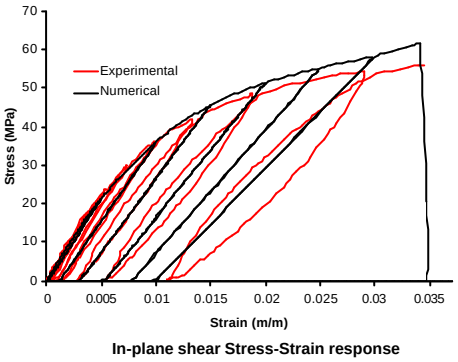

Typical experimental fracture for +45/-45 shear specimen

Band of failed elements in shear

Figure 4. Comparison between experimental and numerical predictions for in-plane shear coupon test

3.2 Impact simulation

The finite element model consists of a 102 × 152 × 3.6 mm^3 rectangular plate with clamped edges impacted by a steel hemispherical impactor under an impact energy of 20 Joules. The mass and diameter of the hemispherical projectile are 2.7 kg and 15.75 mm, respectively. The composite plate has a cross-ply $[(0/90)_2]$ lay-up. The mechanical properties for each composite layer are given in Tab. 1. A surface to surface slide-line contact logic based on the penalty method formulation was defined between the impactor and composite plate. A viscous hourglass algorithm was used to avoid the formation of hourglass modes arising from the use of under integrated elements. Fig.5 shows a comparison between predicted and experimental force histories.

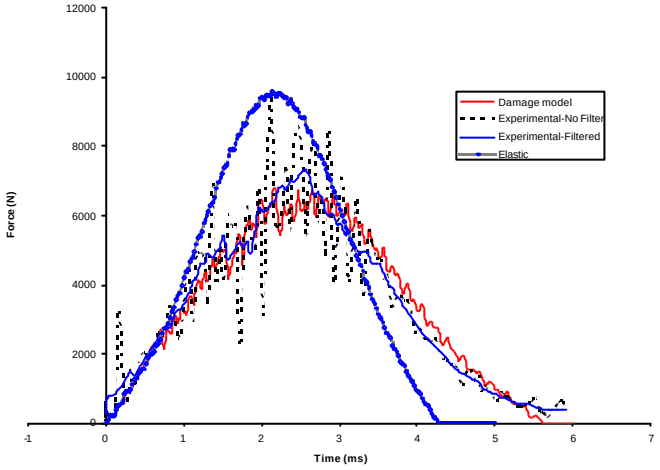

Figure 5. Comparison between experimental and numerical predictions force-time history

It can be seen from Fig. 5 that the numerically predicted failure modes using the proposed damage model correlate remarkably well with the experiments. The experimentally observed failure modes consisted of matrix cracking, delamination and fibre fracture on the bottom face of the specimen due to the high bending stresses on that region. The predicted damage extension also correlates reasonably well with the experiments, as shown in Fig. 6.

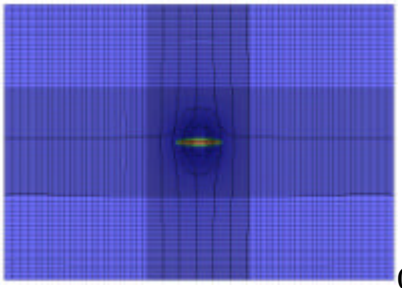

(a)

(b)

Figure 6. Visible damage extension for impacted X-ply specimen: (a) Numerical prediction, (b) Experiment

4. Conclusions

A progressive failure methodology for modeling composite structures under impact loading is presented and discussed in this paper. The proposed formulation enables the prediction of in-plane failure modes in composites within an energy based framework. The accuracy of the model has been checked by comparing numerical predictions with experimental results in different loading ranges varying from static to dynamic impact loading. The model also predicts most of the features experimentally observed including fracture plane direction and damage extension. Due to the similarity in terms of the formulation, the model can be easily combined with decohesion interface elements to predict delamination in composite laminates. Investigation on the validity of the bi-linear constitutive law for predicting damage extension due to fibre kinking propagation and matrix micro-cracking is still under way.

5. Acknowledgements

The authors acknowledge the financial support received for this work from the Brazilian National Research Council (CNPq), contract number 200863/00-2(NV).

6. References

Abrate S., 1991, "Impact on laminated composite materials", Appl. Mech. Rev., Vol. 44, No.4, pp. 155-190.

Abrate S., 2001, "Modeling of impact on composite structures, Composite Structures, Vol. 51, pp. 129-138.

Bazant Z. P., 1983, "Crack band theory for fracture of concrete", Materiaux et Constructions, Vol. 16, pp. 155-177.

Crisfield M.A., Mi Y., Davies G.A.O., 1998, "Progressive delamination using interface elements", Journal of Composite Materials, Vol.32, No. 14, pp. 1247-1271.

Chaboche, J.L., 1988, "Continuum damage mechanics I – General Concepts", J. Appl. Mech., Vol. 55, No 1., pp. 59-64.

Davies G.A.O, Olsson R., 2004, "Impact on composite structures", The Aeronautical Journal, pp. 541-563.

Davies G.A.O, Robinson P., 1992, "Impactor mass and specimen geometry effects in low velocity impact of laminated composites", Int. J. Impact Eng., Vol.12, No. 2, pp. 189-207.

Donadon, M.V., Hodgkinson J., Falzon B.G., Iannucci L., 2004a, "Impact damage in composite structures manufactured using Resin Infusion under Flexible Tooling (RIFT) Process, Proc. 11th ECCM-11, Rhodes, Greece.

Donadon M.V., Hodgkinson J., Falzon B.G., Iannucci L., 2004b, "The reliability of the Resin Infusion under Flexible Tooling process for manufacturing composite aerostructures, Proc. 15th SICOMP, Gothenburg, Sweden.

Donadon M.V., 2005, "Fracture behaviour of unbalanced plain weave fabrics", Internal Report, Dept. of Aeronautics, Imperial College London.

Hashim Z., 1980, "Failure criteria for unidirectional fiber composites", J. Appl. Mech., Vol. 47, pp. 329-334.

Iannucci, L., 2004, "Progressive failure modeling of woven carbon composite under impact", Int. J. Impact Eng. (Article in Press, Corrected Proof).

Jones R.M., 1999, "Mechanics of composite materials", Taylor and Francis, Inc, 2nd edition.

Johnson A.F., 2001, "Modelling fabric reinforced composites under impact loads, Composites, Vol. 32, pp. 1197-1206.

Kachanov L.M., 1958, "Time of rupture process under creep conditions", Izy Akad Nank S.S.R. Otd Tech Nauk, Vol. 8, pp. 26-31.

Ladeveze P., Dantec E. Le, 1992, "Damage modeling of the elementary ply for laminated composites, Comp. Science and Technology, Vol. 43, pp. 257-267, 1992.

Matthews F.L., Soutis C., Smith F.C., 2000, "Predicting the compressive engineering performance of carbon fibre-reinforced plastics, Composites Part A: Applied Science and Manufacturing, Vol. 31, pp. 531-536.

Olsson, R., 2001, "Analitical prediction of large mass impact damage in composite laminates, Composites Part A: Applied Science and Manufacturing, Vol. 32, pp. 1207-1215.

Olsson, R., Donadon M.V., Falzon B.G., 2005, "Delamination threshold load for dynamic impact on plates, Int. J. Solids & Structures (article revised in april 2005 and submitted for publication).

Olsson M.D., Varizi R., Anderson D.L., 1992, "Damage in composites: A plasticity approach", Vol. 44, pp. 103-116.

Oliver J., 1989, "A consistent characteristic length for smeared cracking model", Int. J. for Num. Methods in Eng., Vol. 28, pp 461-474.

Puck A., Shurmann H., 2002, "Failure analysis of FRP laminates by means of physically based phenomenological models", Composite Science and Technology, Vol. 62, pp. 1633-1662.

Rabotnov Y.N., 1968, "Creep rupture", Proc. XII Int. Cong. Appl. Mech.

Williams V. K., Varizi R., Poursartip A., 2003, "A physically based continuum damage mechanics model for thin laminated composite structures, Int. J. Solids & Structures, Vol. 40, pp. 2267-2300.

7. Responsibility notice

The author(s) is (are) the only responsible for the printed material included in this paper.